Control of Global Behavior of FRC Plasmas

S. Okada, K. Yamanaka, S. Yamamoto, N. Iwasawa, K. Kitano, T. Asai, F. Kodera, M. Inomoto, S.Yoshimura, M. Okubo, S. Sugimoto, S. Ohi, S. Goto
Plasma Physics Laboratory, Graduate school of Engineering, Osaka University, Ymada-oka 2-1, Osaka, 565-0871, Japan

Outline

Feature of FRC plasmas

Parameter range

FIX apparatus

Translation

Axial Compression

Neutral Beam Injection

Low Frequency Wave

Feature of FRC Plasmas

Closed magnetic configuration in open magnetic geometry

Good confinement
Direct Energy Converter

High beta value

$$\langle \beta \rangle = 1 - x_s^2 / 2 \approx 90\%$$
$$(x_s = r_s / r_w)$$

No material structure are linking the plasma

Can be moved along machine axis ; TRANSLAION

FRC plasma

configuration

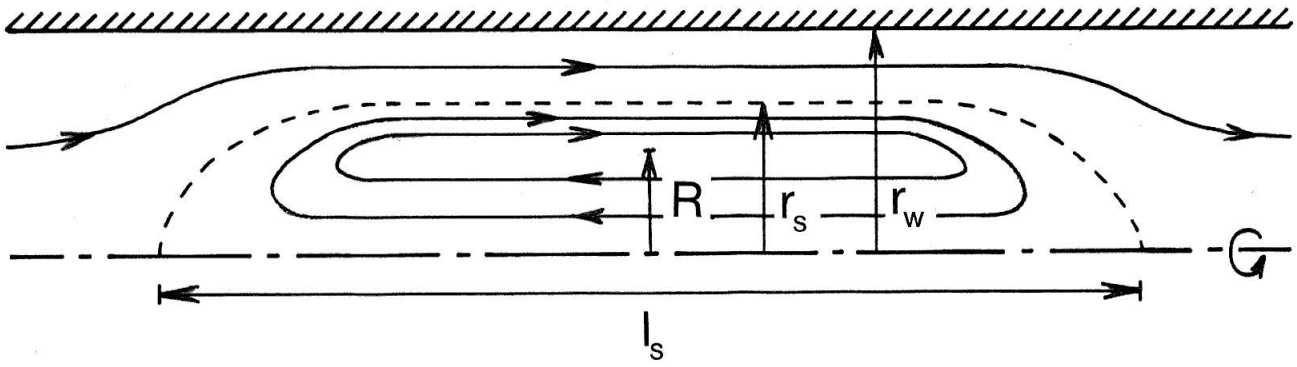

R	magnetic axis radius
r_s	separatrix radius
r_w	conductive wall radius
l_s	length

profiles

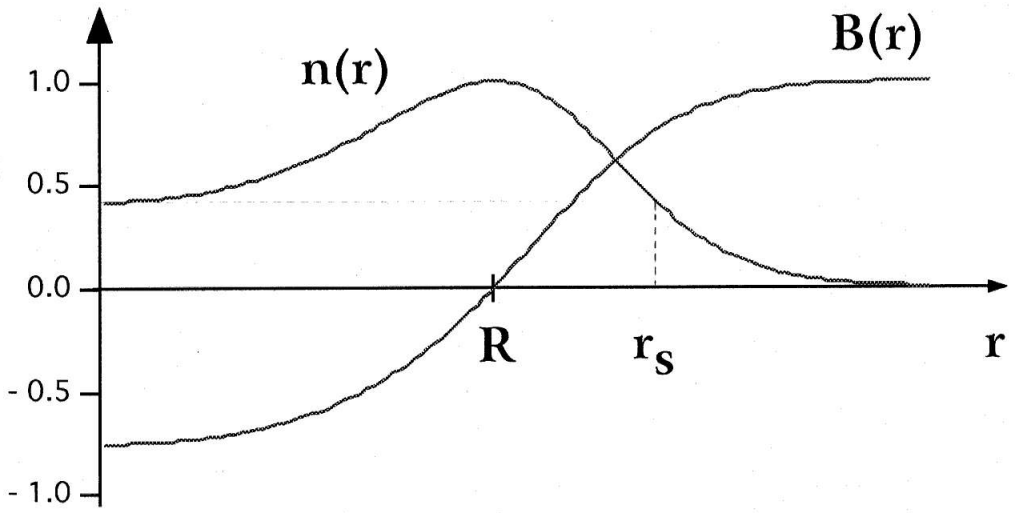

Magnetic field strength to sustain burning plasma

beta value : $\beta = \frac{\text{plasma pressure}}{\text{magnetic pressure}}$

beta limit : stability

	Tokamak (ITER)	FRC	
		ITER equivalent	ARTEMIS D^3He
n_e($10^{20}m^{-3}$)	1.5		5.1
T_i(keV)	17		84
β (%)	6	90	98
B (T)	5.7	1.4	5.4

Parameter Range of FRC Plasmas

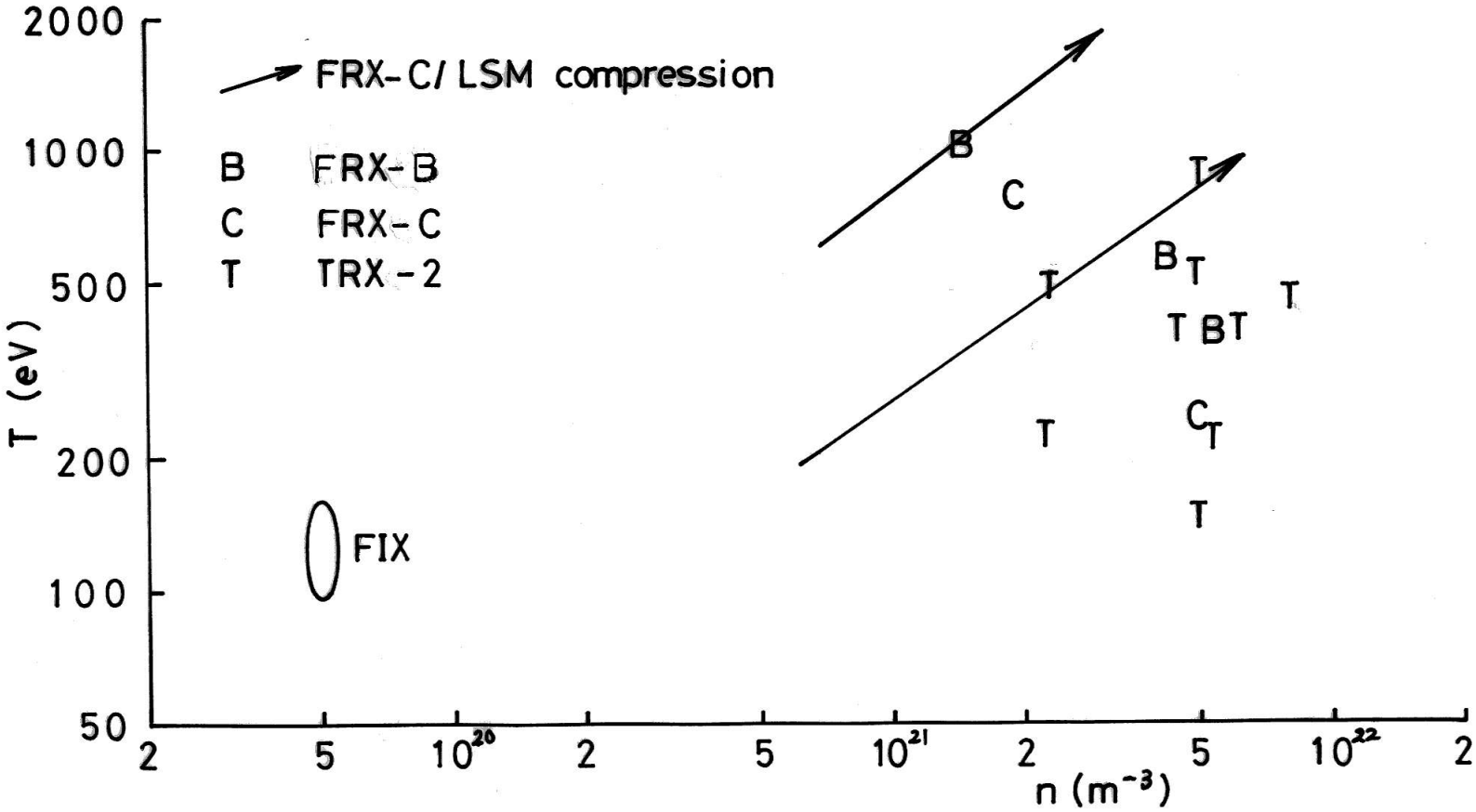

Empirical scaling law

$$\tau_N(sec) = 6.4\times10^{-5} R^2/\rho_i(m)$$

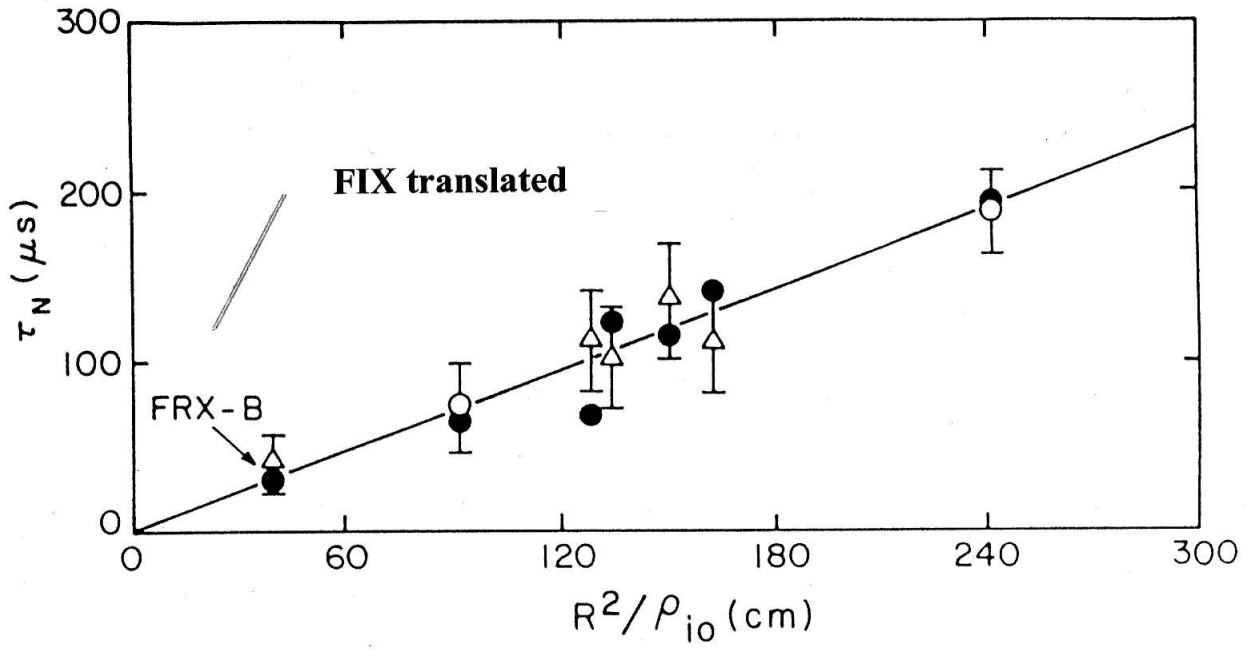

Phys. Rev. Lett. (1983) 1787 McKenna et al.
Phys. Fluids (1984) 1058 Tuszevski et al

Change of plasma length by translation

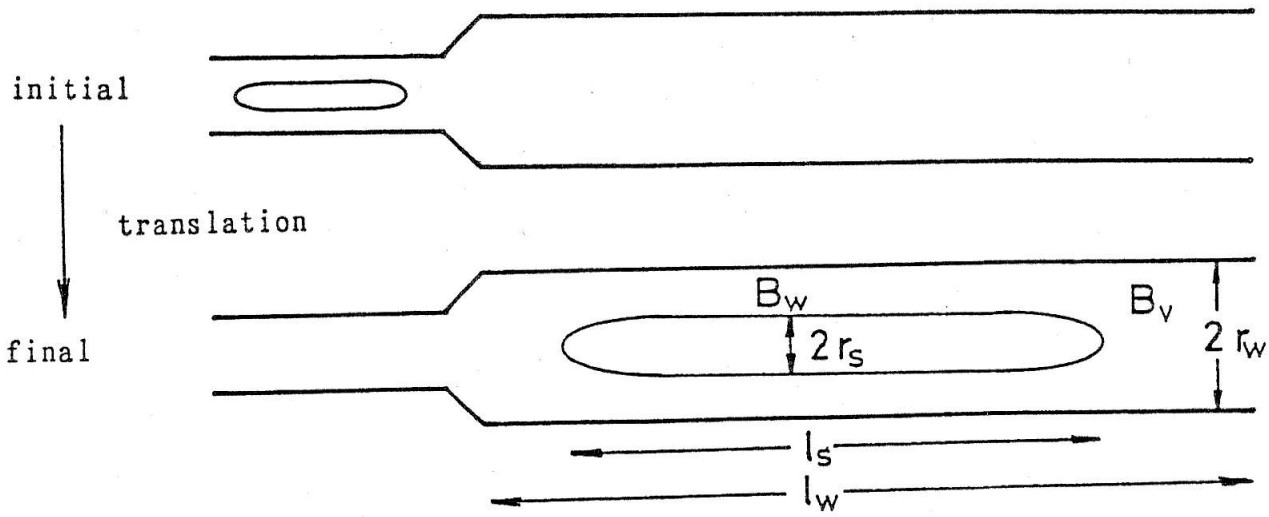

Particle Inventory $N = \pi r_s^2 l_s \langle n \rangle$

Total Energy $E = \frac{5}{2} N\kappa T + \pi r_w^2 l_w \frac{B_v^2}{2\mu_0}$

Trapped Flux $\Phi = \frac{\alpha}{2\sqrt{2}} x_s^3 \pi r_w^2 B_w$

Conservation/Loss $Q_f = (1-\varepsilon_f) Q_i$

$(Q = N, E, \Phi)$

Change of plasma length

$$\frac{l_{sf}}{l_{si}} = \frac{1-\varepsilon_E}{(1-\varepsilon_\Phi)^2} \left(\frac{\beta_f}{\beta_i}\right)^{-1} \left(\frac{\alpha_f}{\alpha_i}\right)^2 \left(\frac{r_{wf}}{r_{wi}}\right)^2 \left(\frac{x_{sf}}{x_{si}}\right)^4$$

Translation Dynamics

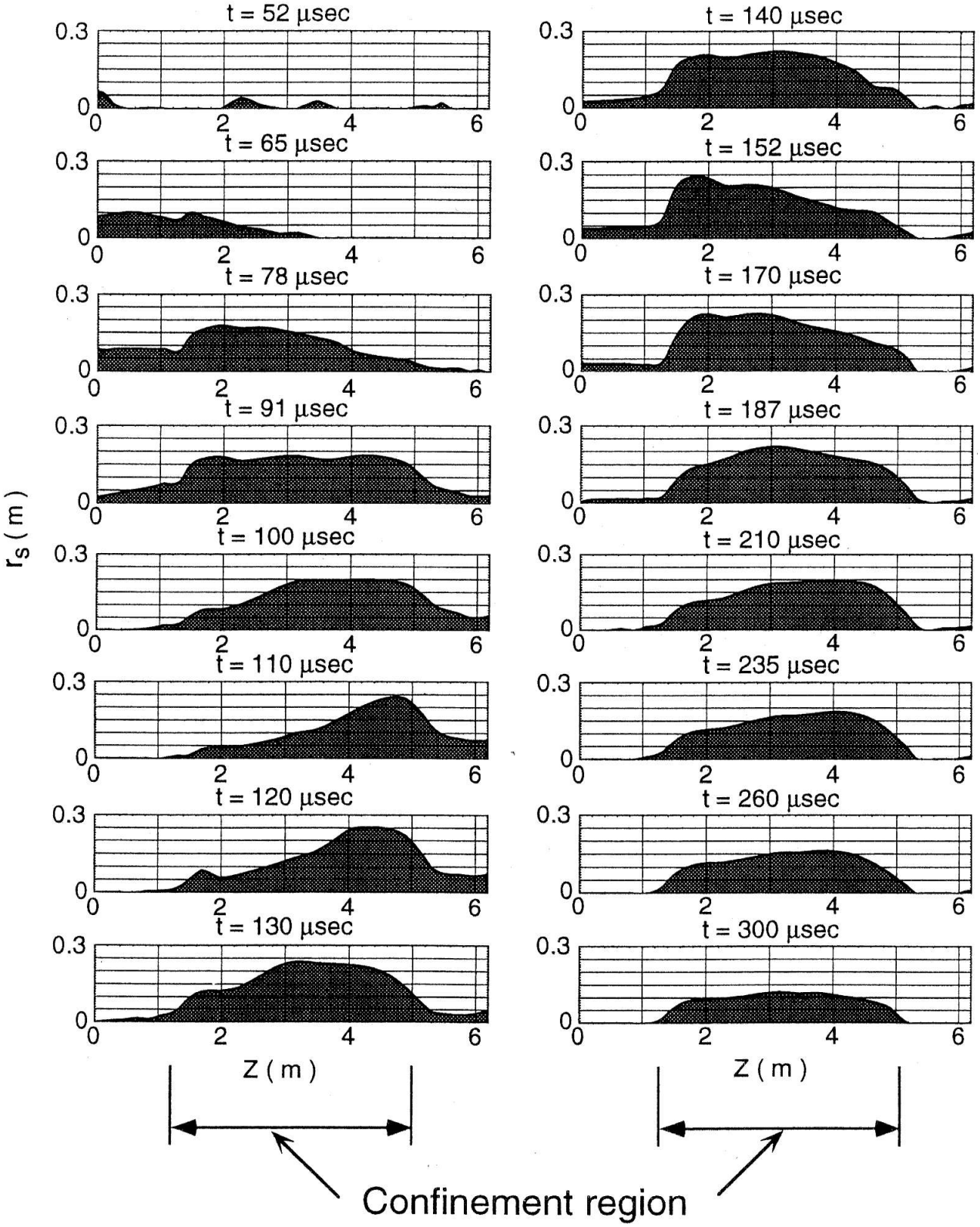

RETHERMALIZATION

$E_B = \frac{2}{2} N\kappa T$ (equilibrium in a straight solenoid)

$E_p = \frac{3}{2} N\kappa T$

Energy Conservation

$\frac{5}{2} N\kappa T + \frac{1}{2} mNv^2 = const$ (no loss)

if $v = 0$ and $N = const$

then $T = const$

Change in temperature with time

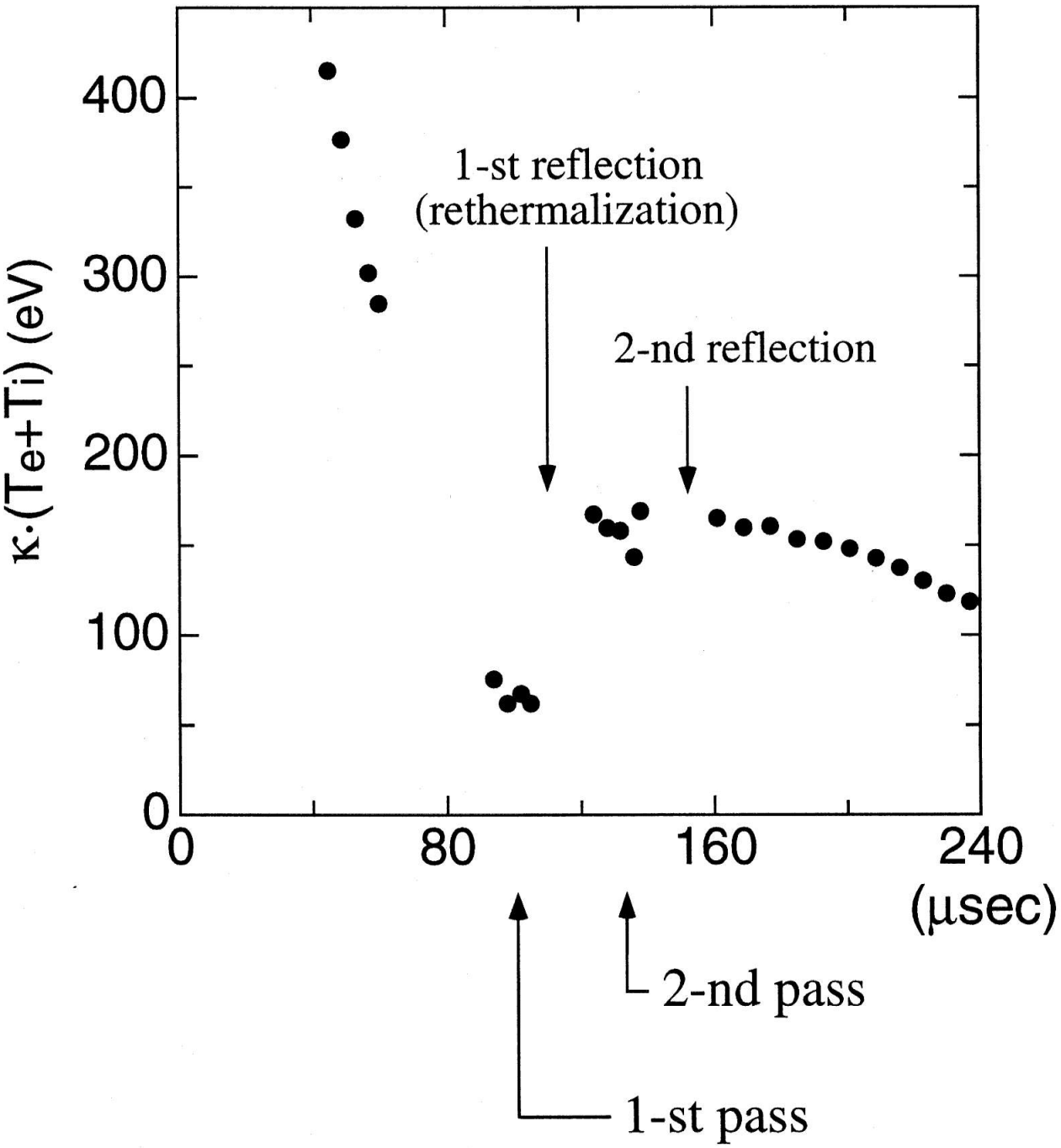

Density after Translation

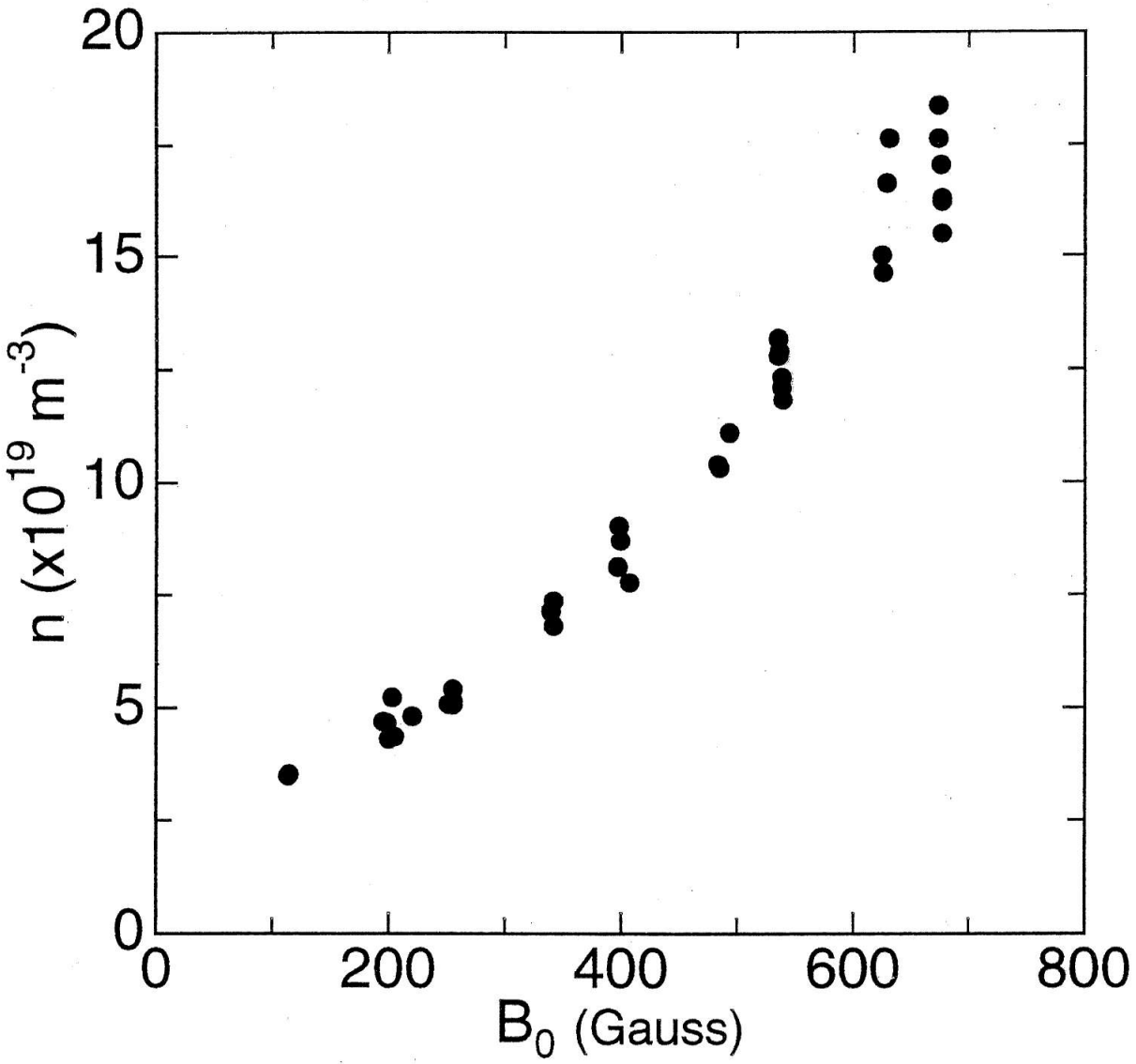

Dependence of Confinement Times on Bias Field

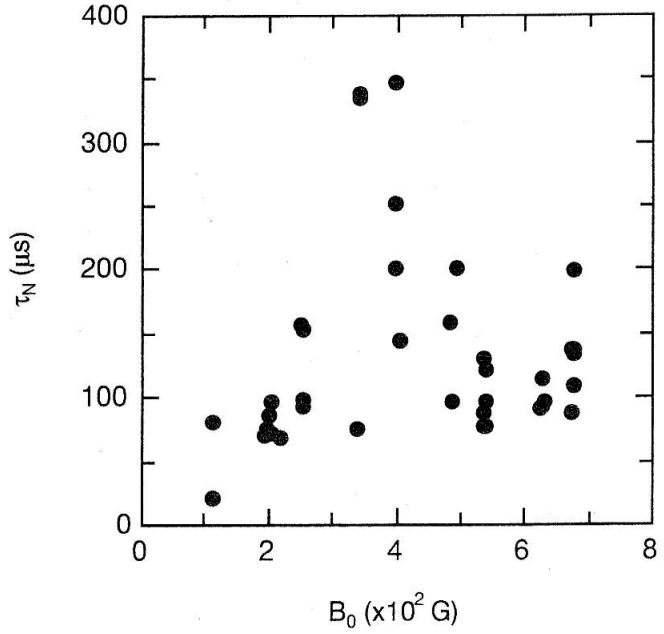

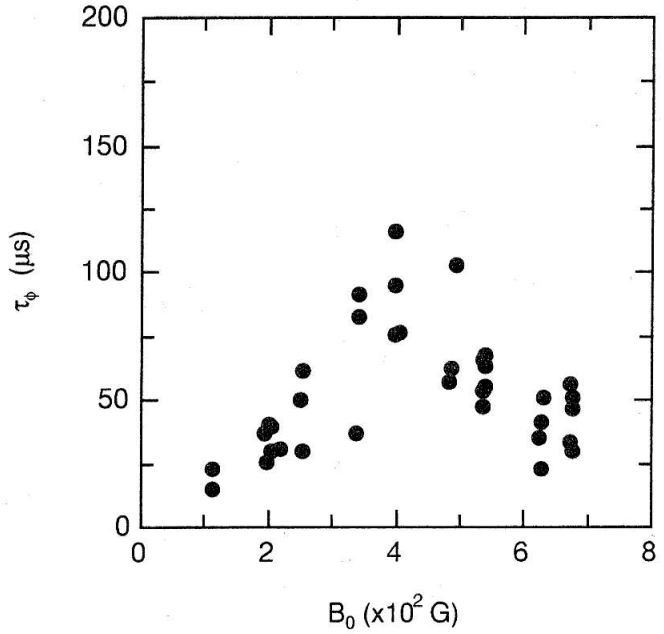

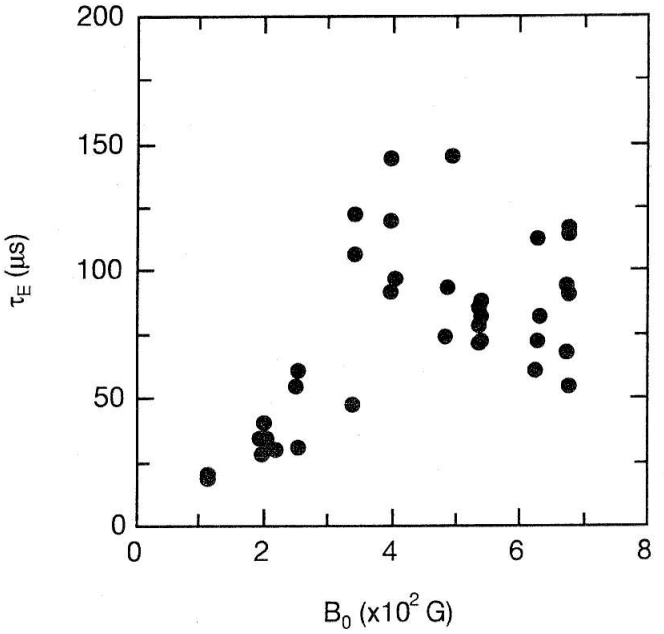

Compression Schemes

3-D

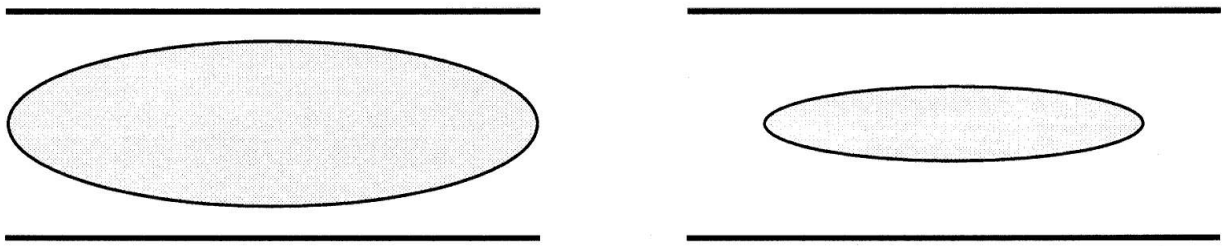

2-D

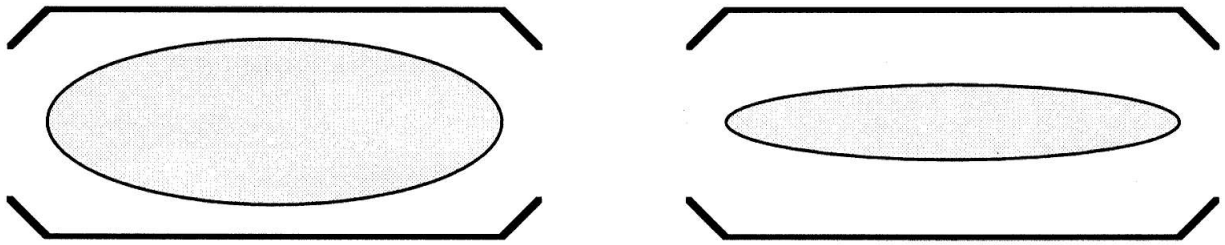

1-D

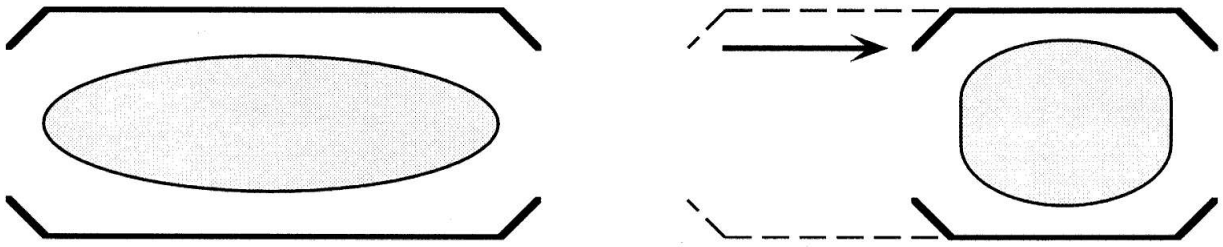

Compression Schemes

	3-D	2-D	1-D
$n_{\max}$	$C^{\frac{2}{\gamma}}$		
T_{tot}	$C^{2\left(1-\frac{1}{\gamma}\right)}$		
ρ_i	$C^{-\frac{1}{\gamma}}\left(\frac{r_f}{r_i}\right)^{\frac{1}{2}}$		
X_s	$C^{-\frac{1}{3+\varepsilon}}$	$C^{-\frac{1}{\gamma}}\left(\frac{\langle\beta\rangle_f}{\langle\beta\rangle_i}\right)^{-\frac{1}{2}}$	$Eq.$
l_s	$C^{\frac{2}{3+\varepsilon}-\frac{2}{\gamma}}\left(\frac{\langle\beta\rangle_f}{\langle\beta\rangle_i}\right)^{-1}$	1	$\frac{l_{sf}}{l_{si}}$
V	$C^{-\frac{2}{\gamma}}$	$C^{-\frac{2}{\gamma}}\left(\frac{\langle\beta\rangle_f}{\langle\beta\rangle_i}\right)^{-1}$	$C^{-\frac{2}{\gamma}}\left(\frac{\langle\beta\rangle_f}{\langle\beta\rangle_i}\right)^{-1}$
τ	$C^{\frac{1}{\gamma}-\frac{2}{3+\varepsilon}}\left(\frac{r_f}{r_i}\right)^{-\frac{1}{2}}$	$C^{-\frac{1}{\gamma}}\left(\frac{\langle\beta\rangle_f}{\langle\beta\rangle_i}\right)^{-1}\left(\frac{r_f}{r_i}\right)^{-\frac{1}{2}}$	$\left(\frac{X_{sf}}{X_{si}}\right)^2 C^{\frac{1}{\gamma}}\left(\frac{r_f}{r_i}\right)^{-\frac{1}{2}}$

compression ratio $\quad C = B_{W2}/B_{W1}, \qquad C = R^{\gamma/2}$

density ratio $\quad R = n_{\max 2}/n_{\max 1}, \qquad R = C^{2/\gamma}$

temperature ratio $\quad r = T_i/T_{tot}$

$Eq.$ $\quad \frac{1-X_{sf}^2}{1-X_{si}^2} = \left(\frac{\langle\beta\rangle_f X_{sf}^2 l_f}{\langle\beta\rangle_i X_{si}^2 l_i}\right)^{\frac{\gamma}{2}}$

Axial Compression

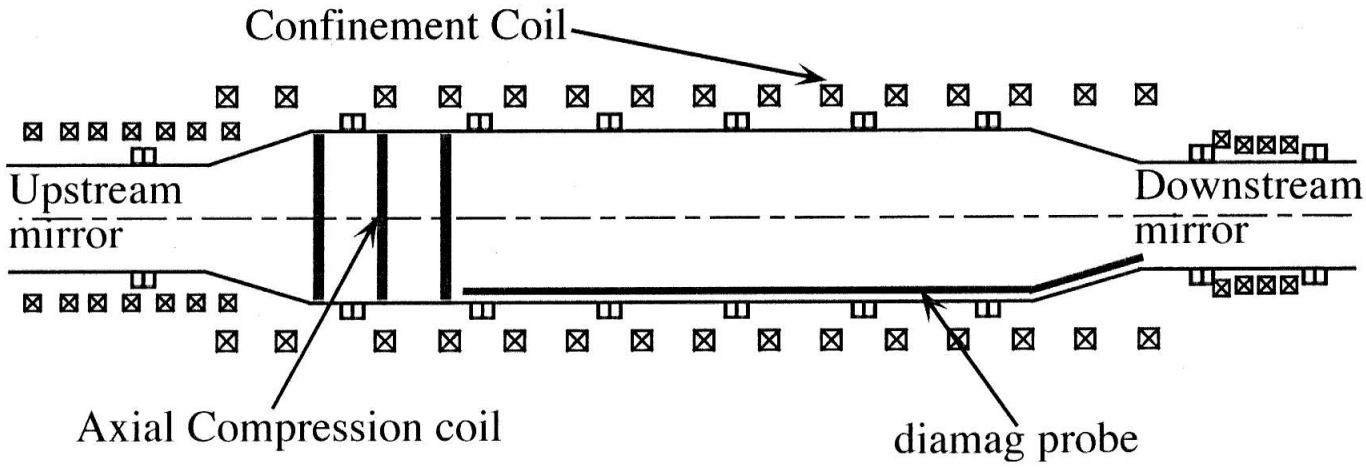

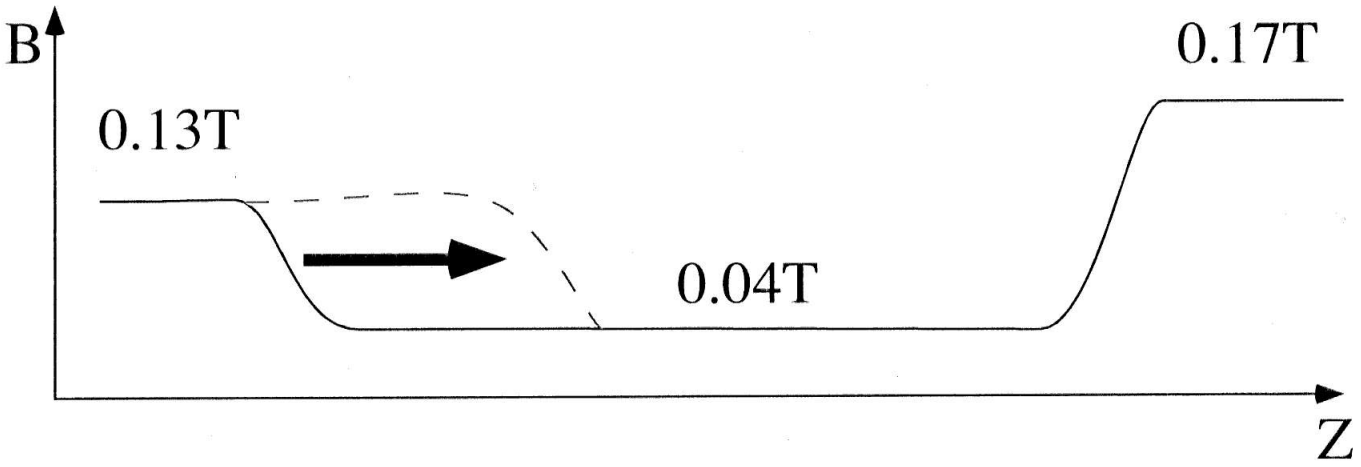

Change of x_s by axial compression

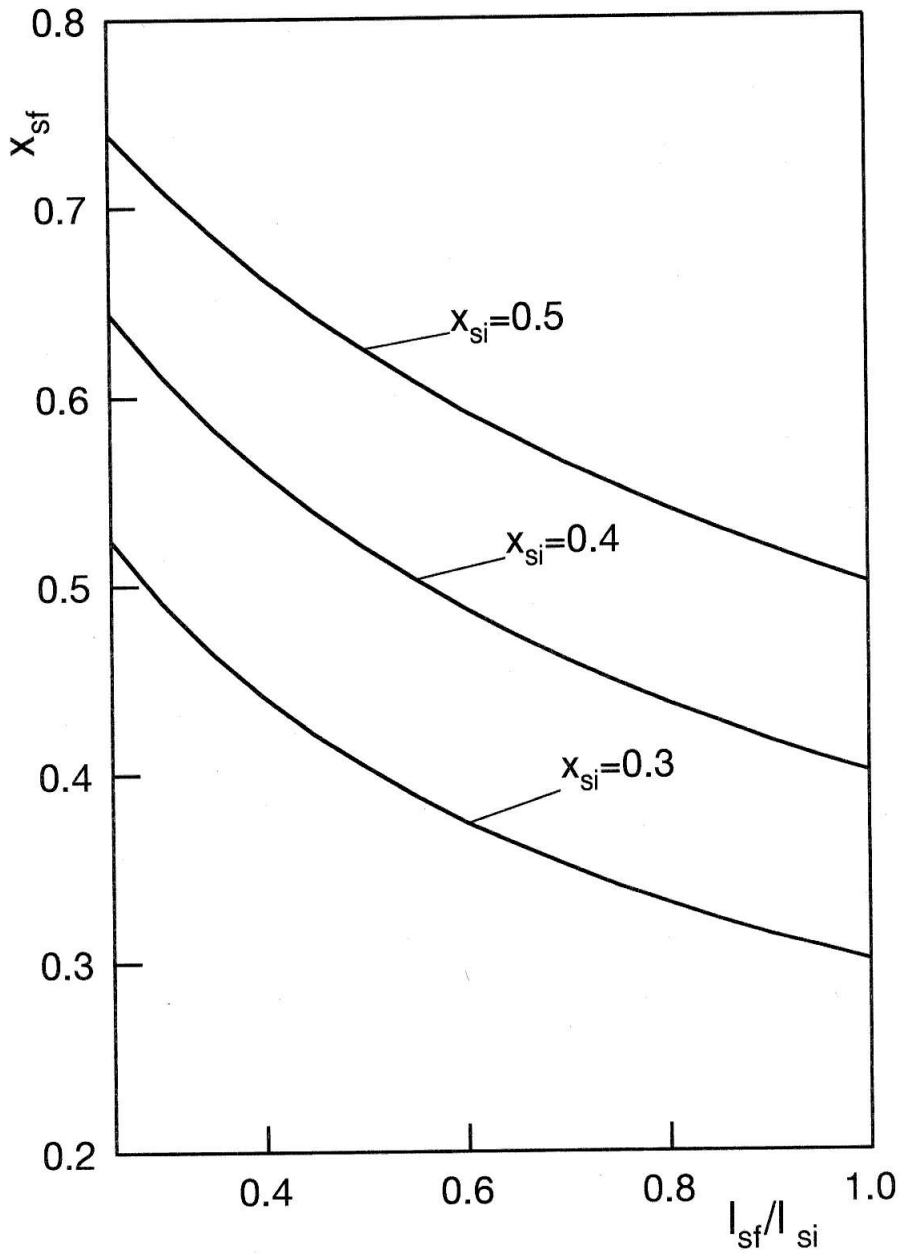

Heating by axial compression

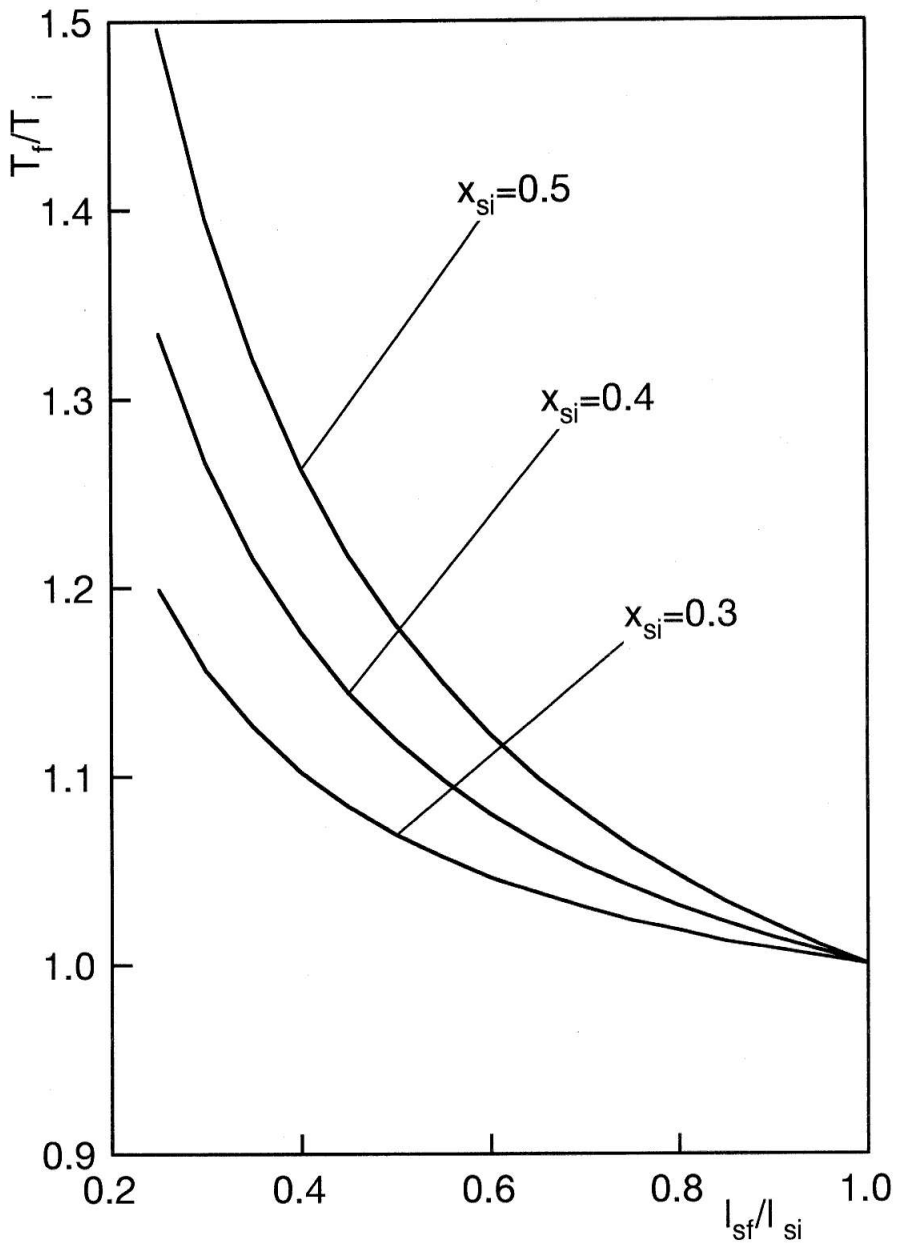

Confinement improvement by axial compression

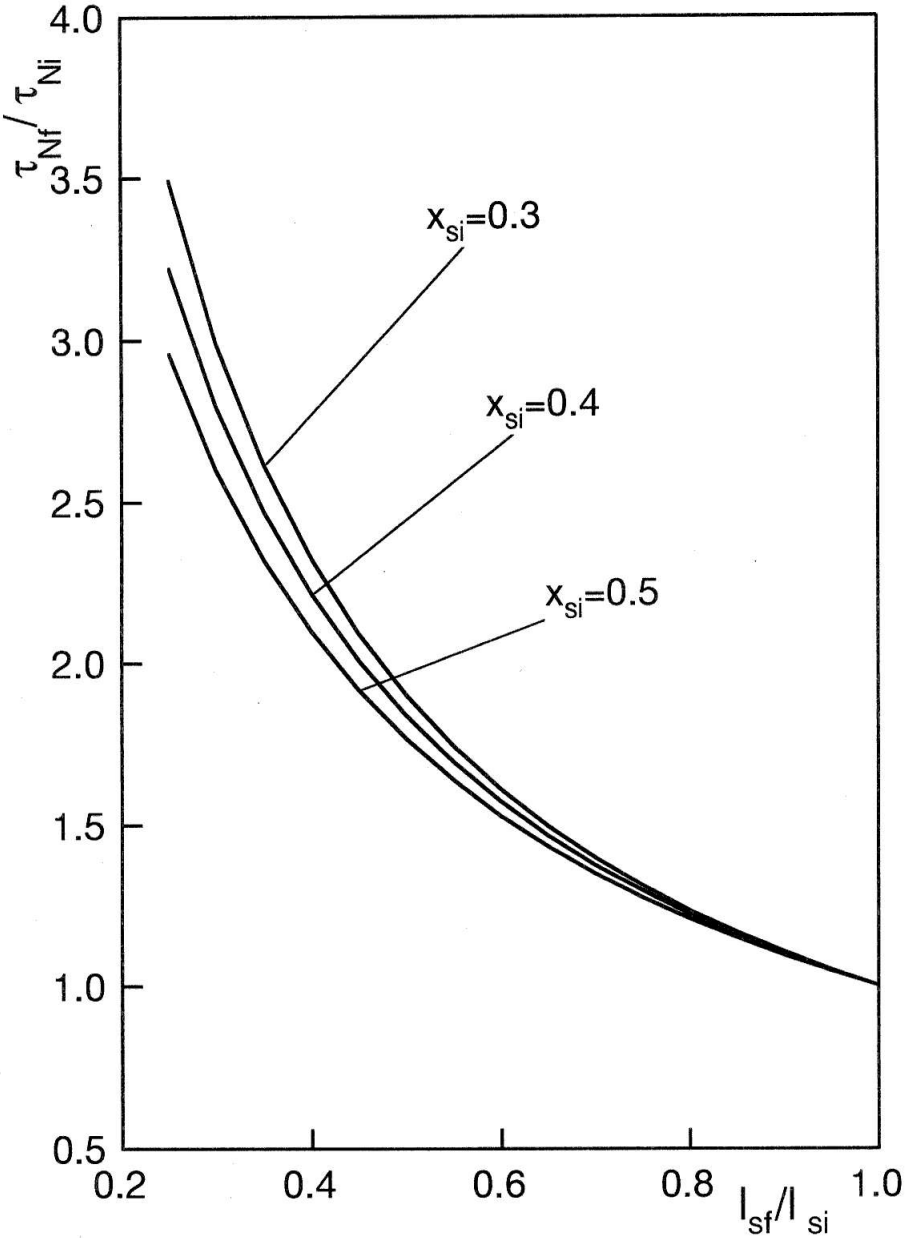

Change of Separatrix radius with Time

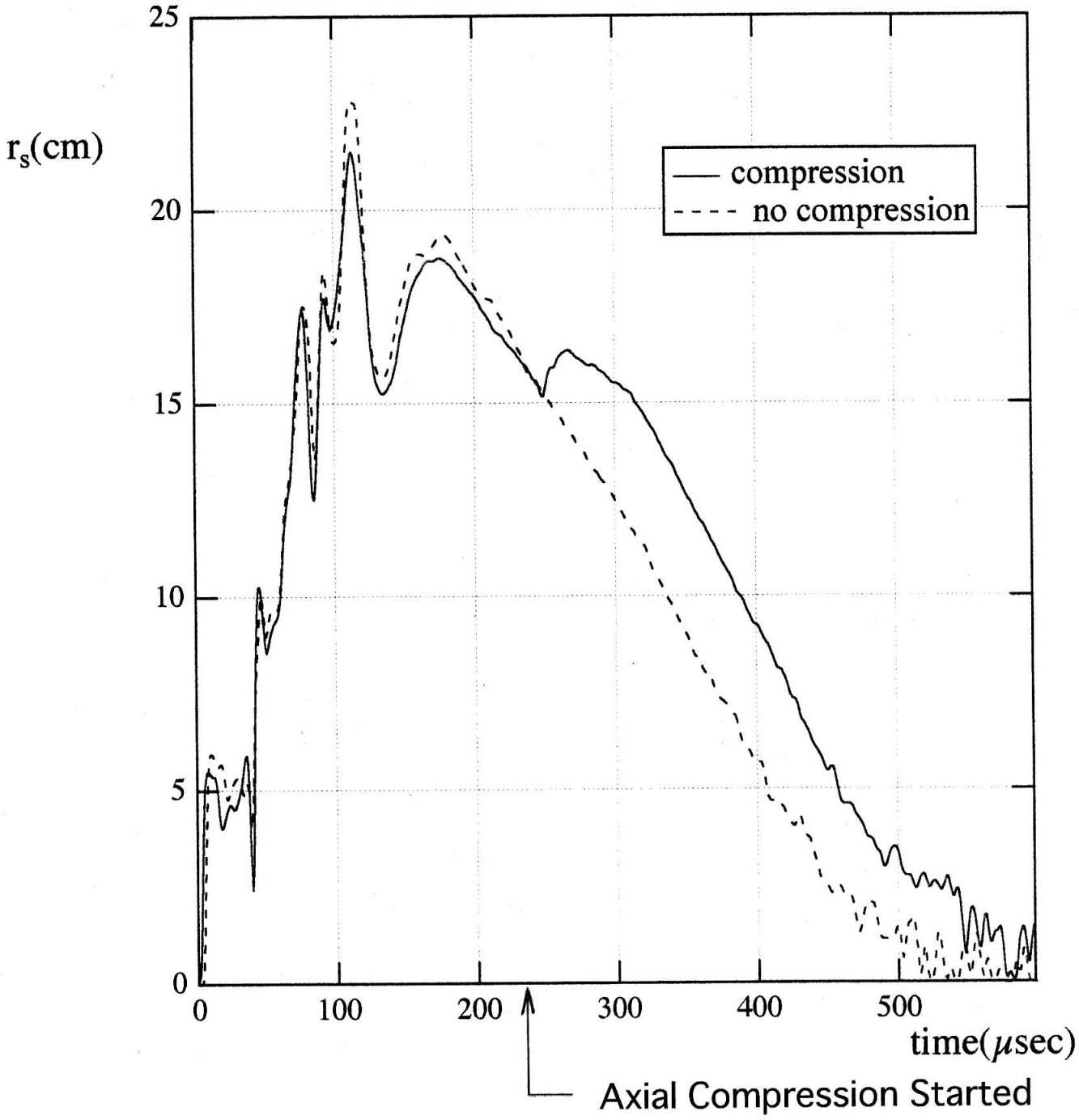

Axial Compression
(Comparison with Empirical Scaling)

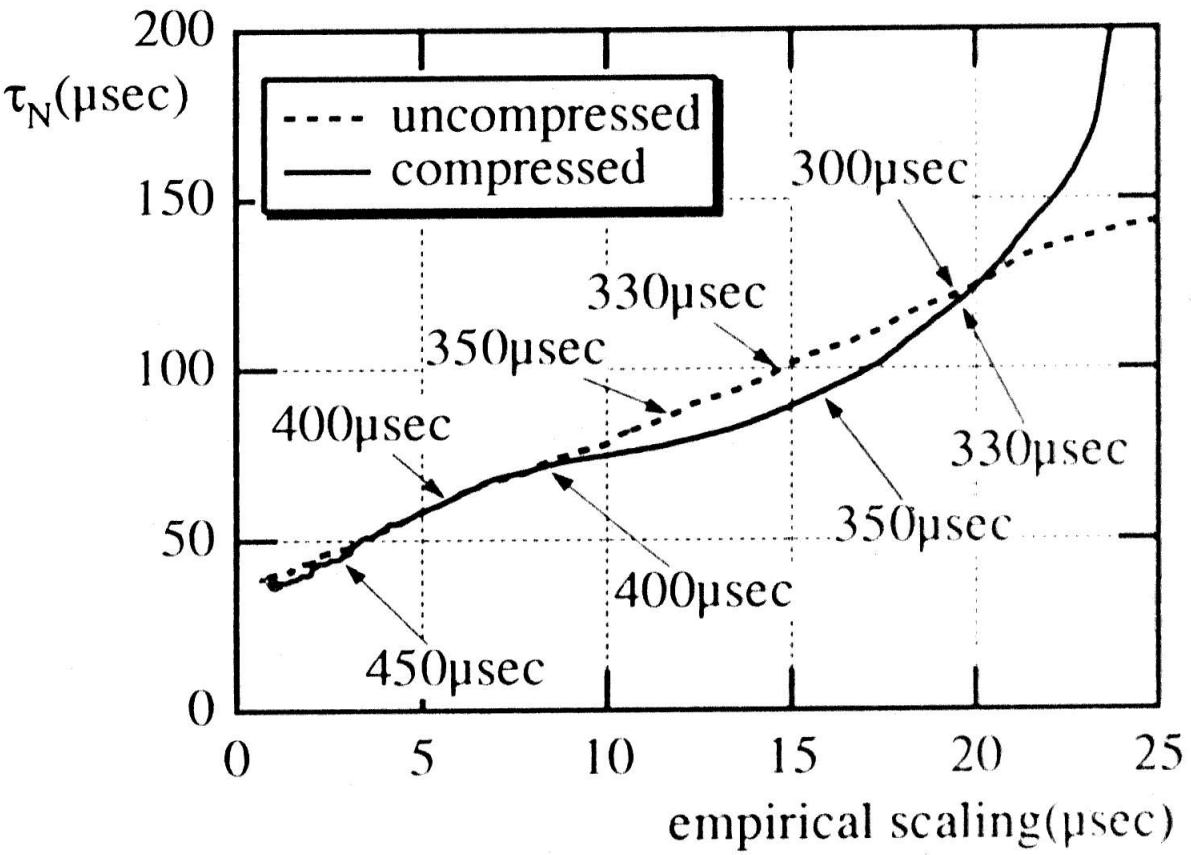

Fig.5 Particle confinement time τ_N at each instance of time plotted against the value calculated for the empirical scaling law with (solid line) and without (dotted line) axial compression. Confinement is improved by bringing the gradually decaying FRC back into a state with larger empirical scaling parametr and larger confiment time τ_N. For example, the point with the time marker 330 μs on the compressed case has larger empirical scaling parameter and therefore larger τ_N than that of the uncompressed case.

Experimental Arrangement for Neutral Beam Injection

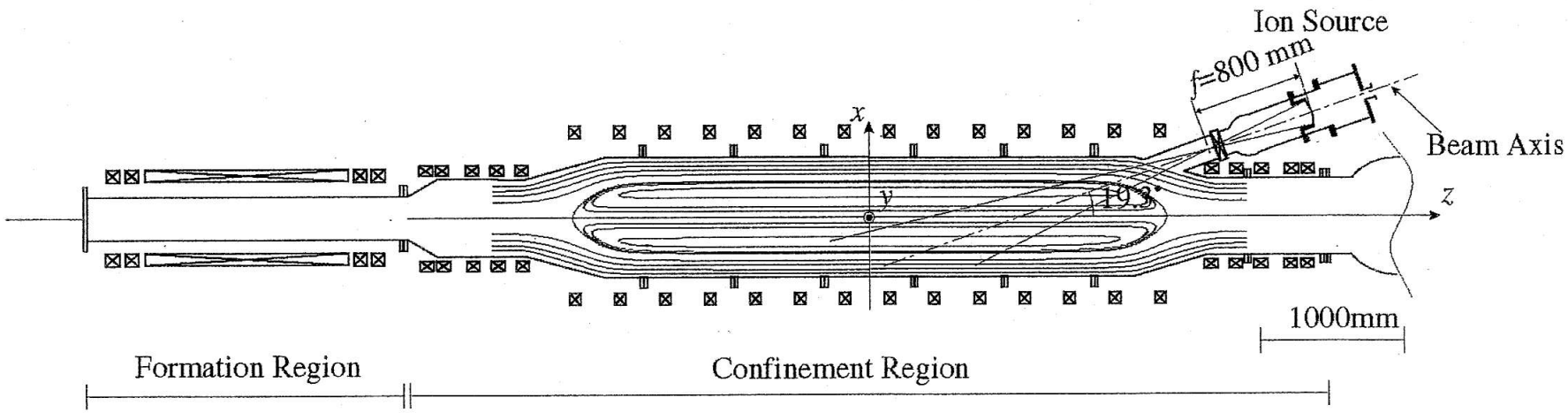

Schematic diagram of the FRC confinement chamber with NB injection system.

Time Evolution of Stored energy

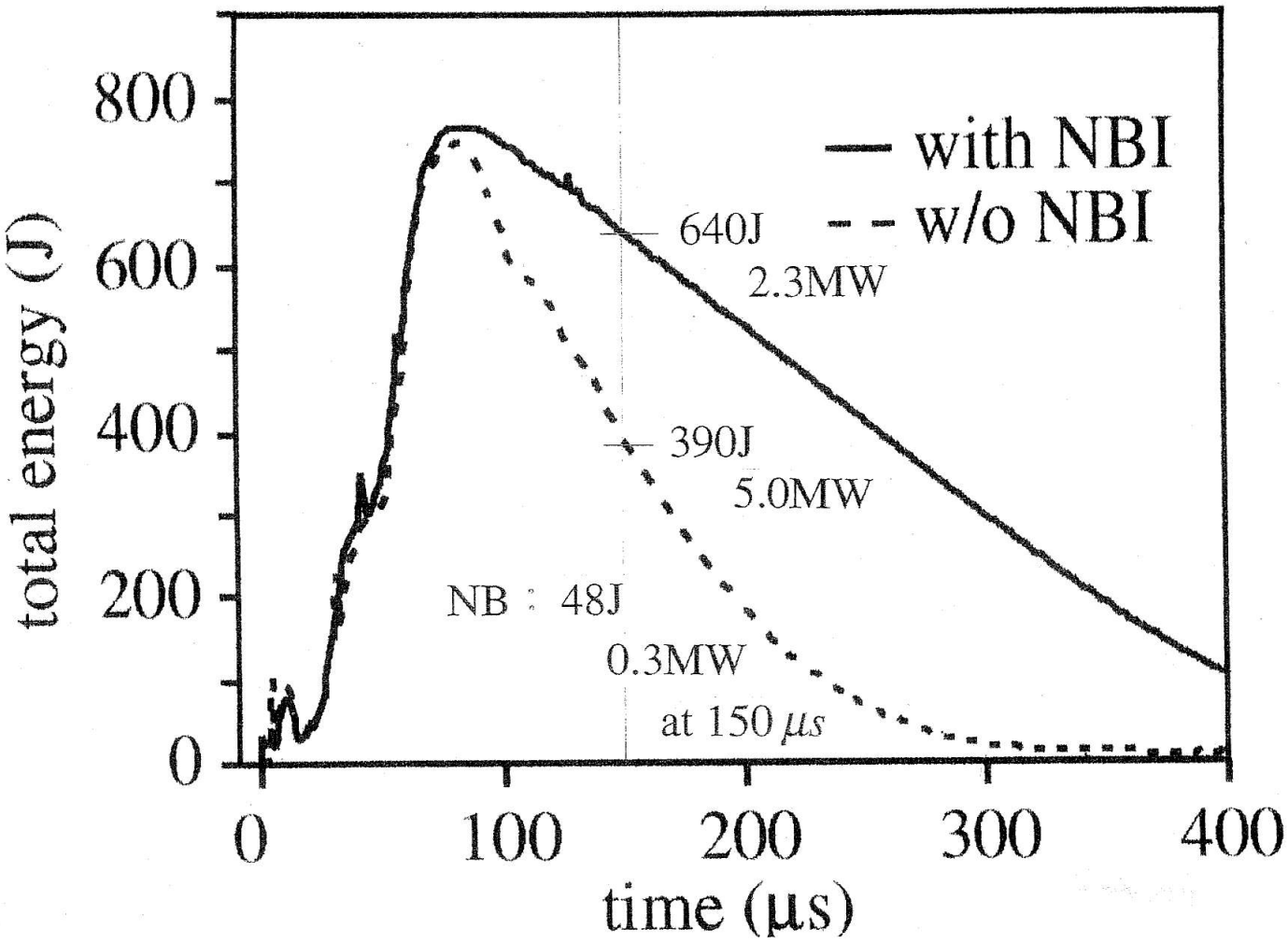

Dependence of Confinement / Confinement Improvement on Mirror Ratio

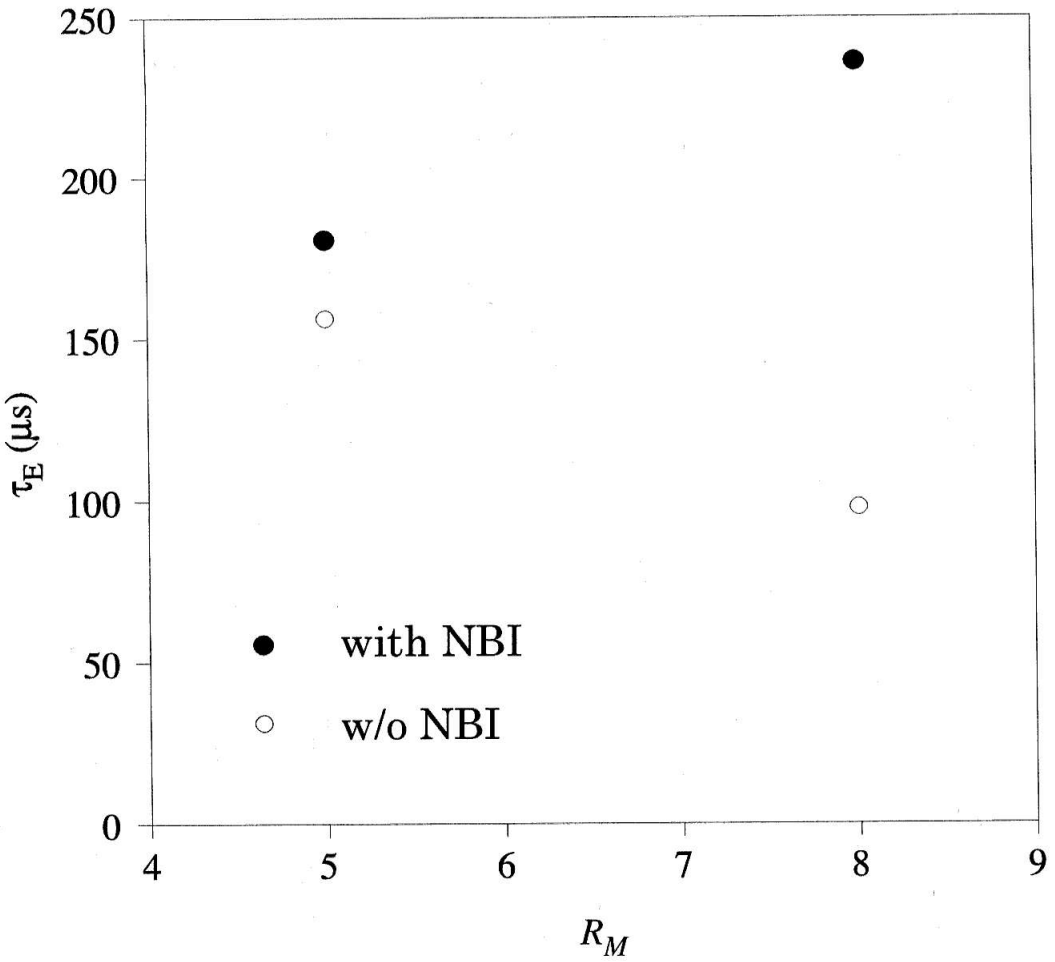

Arrangement for
Low Frequency Wave Experiment

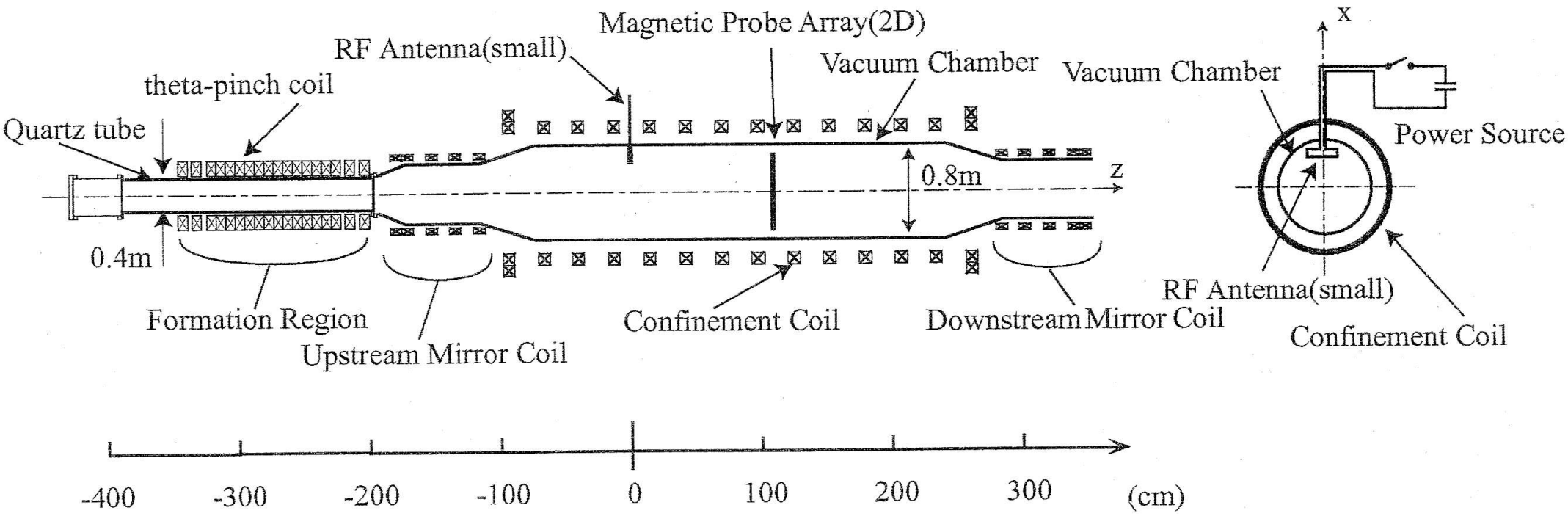

Time Evolution of Stored Energy

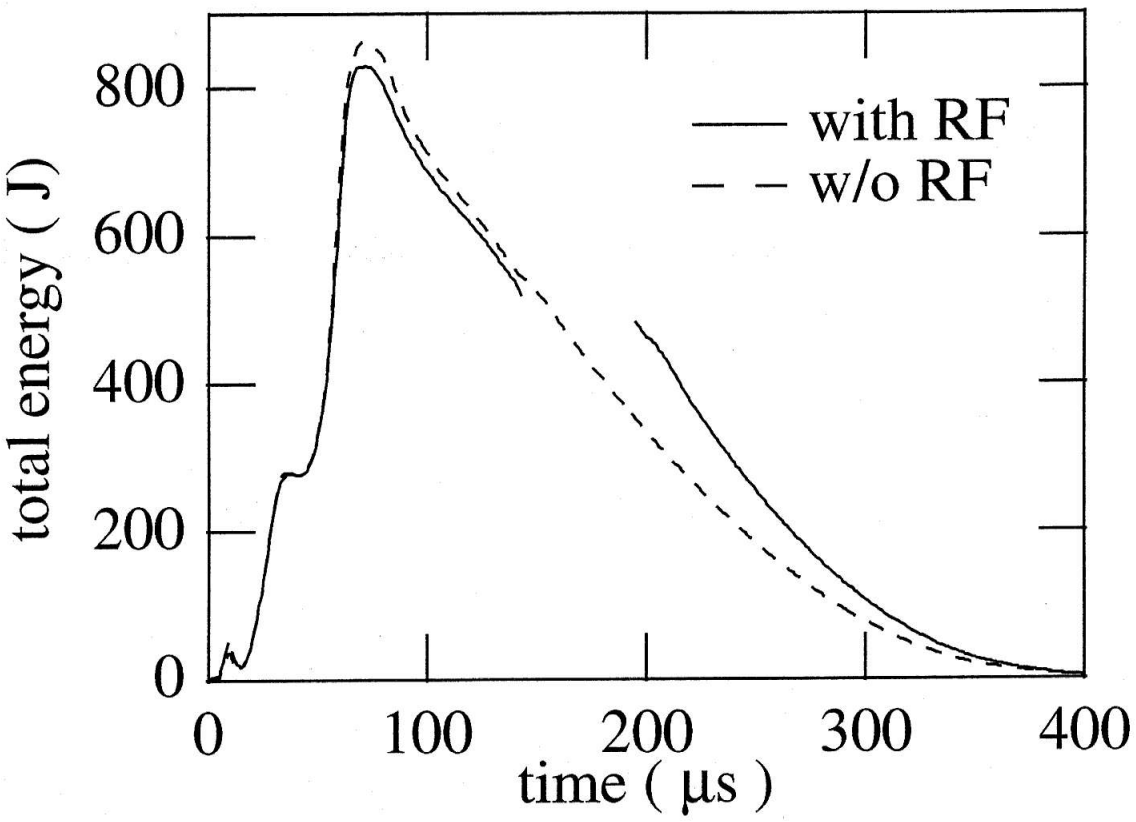

Effects of RF Heating

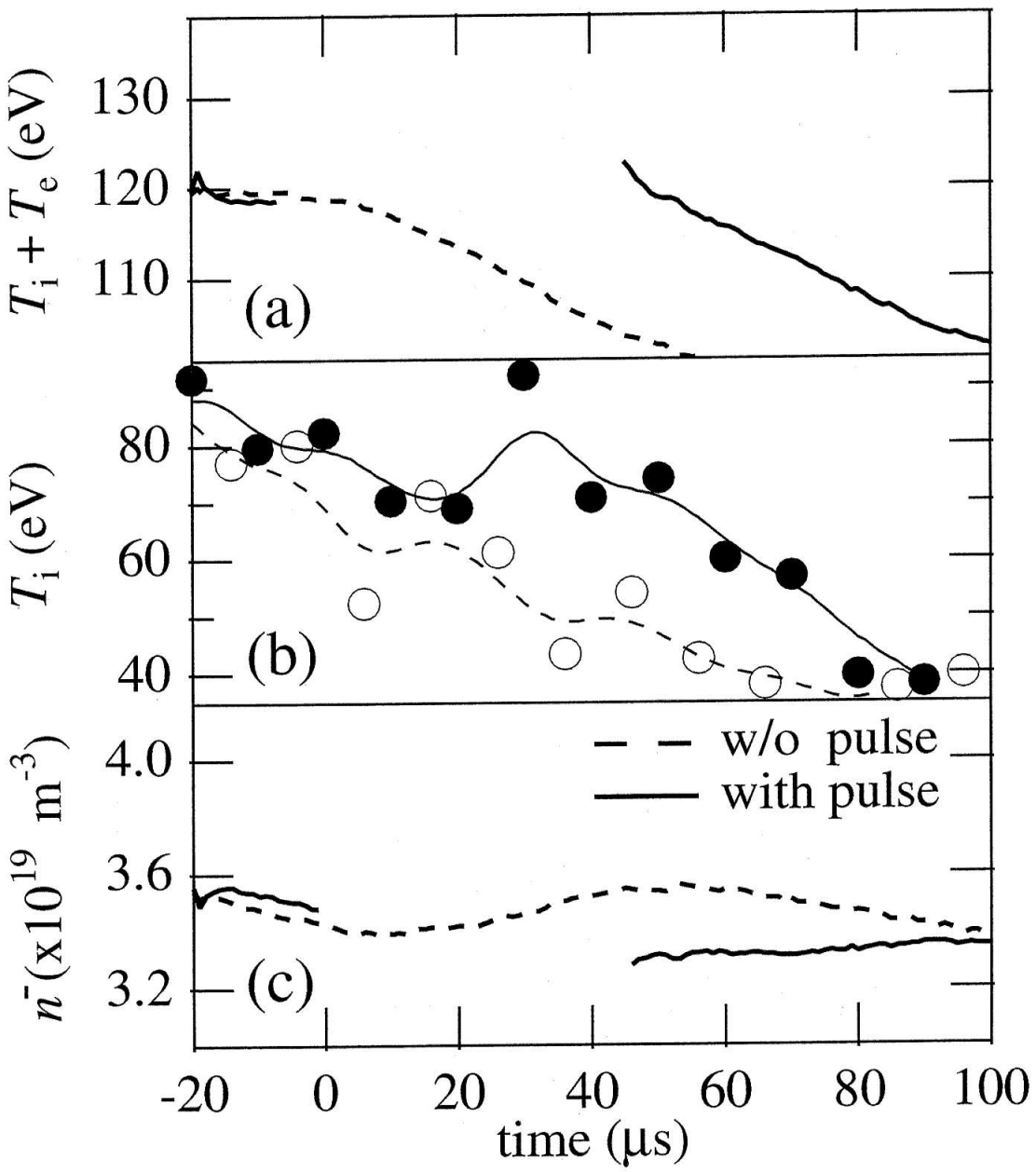

Induced Magnetic Field disturbance

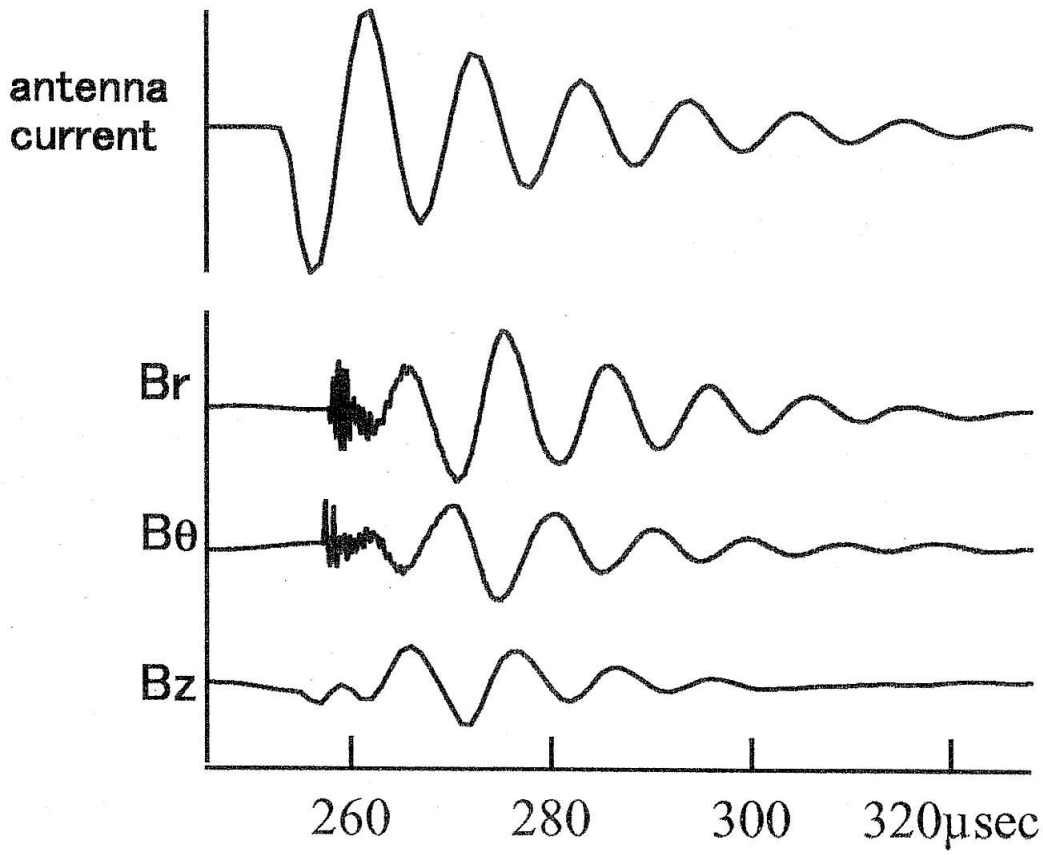

Propagation of Magnetic Disturbances

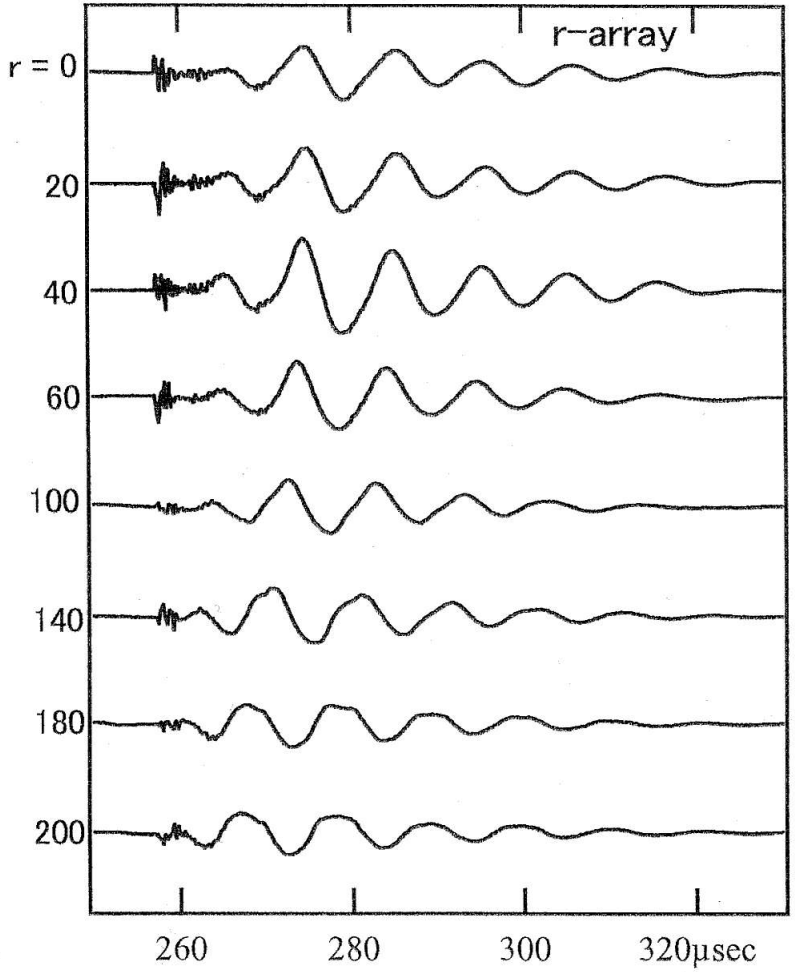

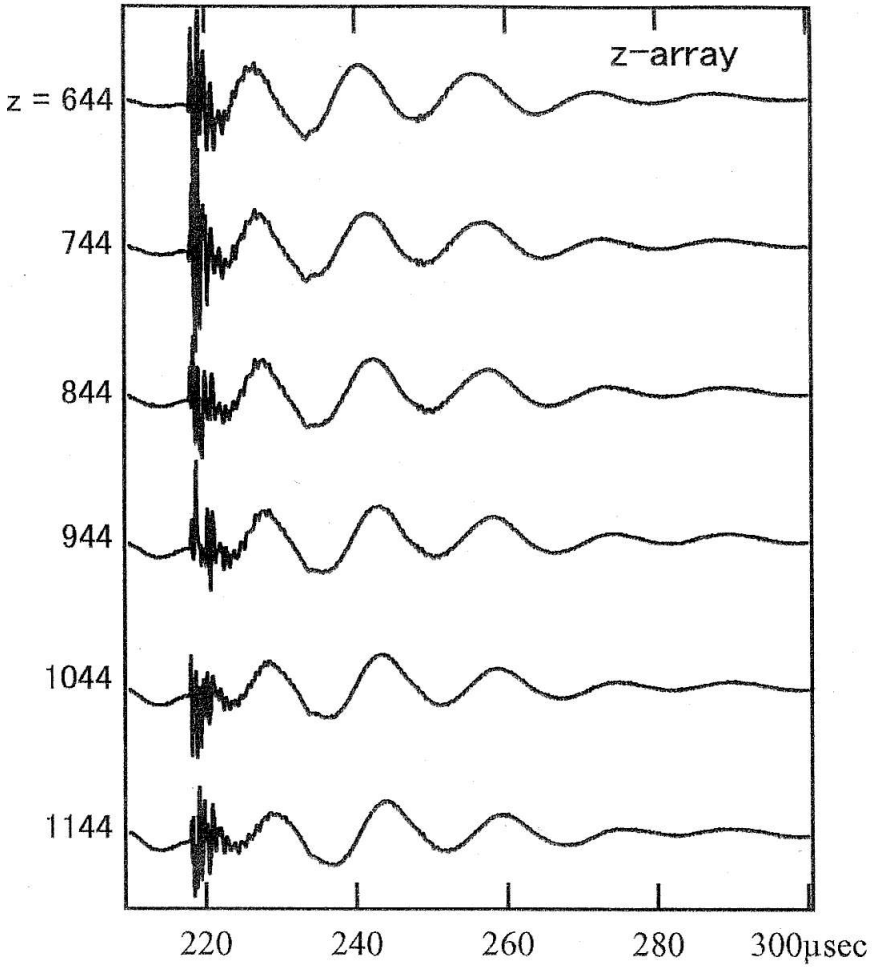

Dispersion Relation of B_θ Disturbance

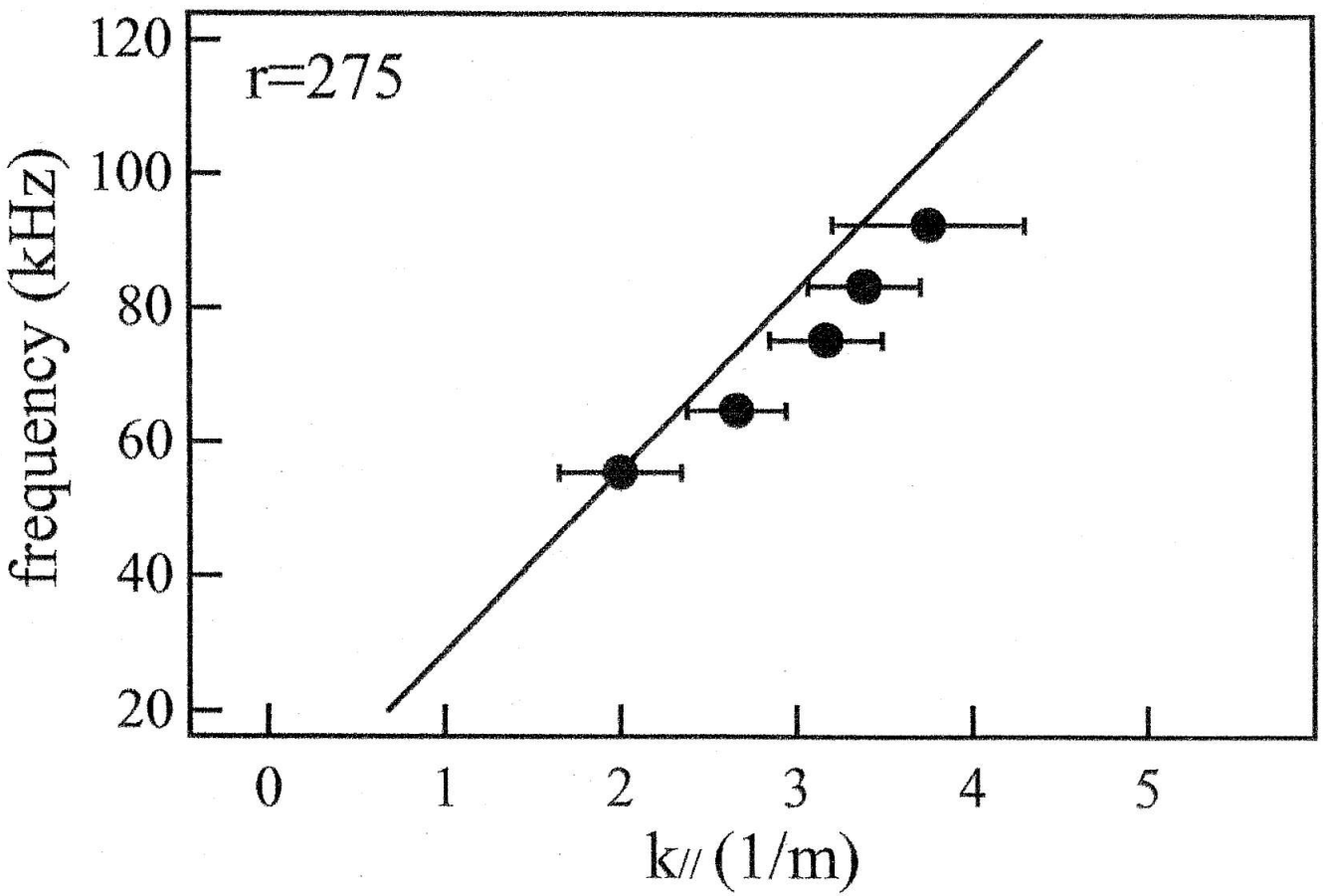

Spatial Variation of v_z